International Core Journal of Engineering Volume 11 Issue 6, 2025
ISSN: 2414-1895 DOI: 10.6919/ICJE.202506_11(6).0019

# Analysis of Mechanical Behavior of Doubler Plate Reinforced CHS-to-SHS T-joint

Zhishen Yuan[a], Yangzhi Zhao[b], Shuchen Gan[c]

College of Civil Engineering, Central South University of Forestry and Technology, Changsha 410004, China

[a]yzs@csuft.edu.cn, [b]1486934583@qq.com, [c]18773189433@139.com

## Abstract

**In order to address the issue of localised plastic damage to CHS-to-SHS T-joint, which occurs as a result of the axial pressure exerted by the branch pipe, an improvement in the bearing capacity of thejoint has been achieved through the welding of a cladding plate to the surface of the main pipe. The finite element model of CHS-to-SHS T-joint was verified based on the results of the tests conducted on the joint. The verification was carried out using the joint load-displacement curve, damage mode and bearing capacity. The verified model was reinforced with the cladding plate, and a finite element parameter analysis was conducted to ascertain the strengthening law of the cladding plate on the joint. Subsequently, a design formula for the bearing capacity of CHS-to-SHS T-joint reinforced with the cladding plate was established through linear regression. The analysis results demonstrate that increasing the thickness, width and length of the cladding plate can enhance the compressive load-bearing capacity of the joint. However, it is observed that the greatest improvement in load-bearing capacity is achieved when the thickness of the cladding plate is increased.When the thickness and width of the cladding plate remain unchanged,the reinforcing effect of the cladding plate with a length ratio of the cladding plate to the main pipe of 1.2 is the best.For the reinforced joints with the same cladding plate size,the enhancement ratio of joint will improve more while the width ratio of branch to main tube ($\beta$) is smaller.The CHS-to-SHS T-joint,reinforced by the cladding plate,may be over-reinforced because of a small or large branch-to-main pipe width ratio ($\beta$) .The results of the formula presented in the paper are in close alignment with the parameter analysis results.**

## Keywords

**Doubler Plate Reinforced CHS-to-SHS T-joint; Bearing Capacity; Parametric Analysis; Correction Factor; Formula Fitting.**

## 1. Introduction

Steel tube structures exhibit excellent mechanical properties and aesthetic architectural effects, making them widely used in spatial structures such as offshore platforms and gymnasiums. However, to form a structural system, steel tubes must be connected through joints, which requires the joints to have reliable load-bearing capacity. Hollow and thin-walled steel tubes feature significantly lower radial stiffness compared to axial stiffness, so the area near the weld on the surface of the main tube is a common failure location in tubular joints [1]. To enhance joint load-bearing capacity, reinforcement of steel tube joints is often necessary. The reinforcement methods for steel tube joints can be divided into internal reinforcement and external reinforcement. Internal reinforcement mainly includes increasing the wall thickness of the main tube, and setting stiffening rings or vertical insert

ISSN: 2414-1895 DOI: 10.6919/ICJE.202506_11(6).0019

plates inside the main tube [2-4], etc.;common external reinforcement methods include welding cover plates [4-11] or ring plates [12-14] on the surface of the main tube. Chang et al.[7] analyzed the compression load-bearing mechanism of cover plate-reinforced T-shaped square steel tube joints and derived a load-bearing capacity formula for cover plate-reinforced joints under axial compression using the plastic hinge line method; Feng et al.[10] performed parameter analysis on cover plate-reinforced square steel tube joints, introduced an improvement coefficient to modify the load-bearing capacity formula for unreinforced square steel tube joints in the European Code, and obtained the compression load-bearing capacity of reinforced square steel tube joints; Soh et al.[11]provided an ultimate load-bearing capacity formula for cover plate-reinforced square steel tube joints under axial compression through linear regression; Wang et al.[12,13] gave the compression load-bearing capacity calculation formula and its applicable range for ring plate-reinforced T-shaped square steel tube joints through axial compression performance tests and finite element parameter analysis; Cai et al.[14] conducted experimental studies on three ring plate-reinforced T-shaped circular steel tube joints and found that ring plate reinforcement can increase the length of plastic hinge lines, thereby improving the joint load-bearing capacity;Li et al.[2] conducted finite element analysis on T-shaped circular steel tube joints strengthened with built-in vertical insert plates, derived the strengthening rules of built-in vertical insert plates for T-shaped circular steel tube joints, and provided the recommended size range for the strengthening insert plates.The above analyses focus on reinforced joints where both the main and branch tubes are square tubes or circular tubes, while there is less research on reinforced joints with square main tubes and circular branch tubes. China's codes [15] mainly provide suggestions for the design of reinforcing plates, but do not give clear load-bearing capacity design formulas.

Therefore, to solve the problem of local plastic failure easily occurring in the main tube wall of T-shaped square main tube and circular branch tube joints under branch tube axial pressure, this paper proposes a method of reinforcing the main tube wall with cover plates to achieve the goal of improving joint compression load-bearing capacity. Through parameter analysis of cover plate-reinforced T-shaped square main tube and circular branch tube joints under branch tube axial pressure, the effects of cover plate dimensions on the failure modes and load-bearing capacity of joints with various geometric parameters are analyzed, and then a compression load-bearing capacity calculation method for this type of reinforced joint is proposed to provide a scientific basis for engineering applications.

## 2. Establishment and Validation of Finite Element Model

### 2.1 Calculation Diagram

Fig. 1 shows the geometric parameter symbols of the cover plate-reinforced T-shaped circular branch tube-square main tube intersecting joint. Here,$L_0$ and $L_1$ are the lengths of the main tube and branch tube, respectively;$b_0$ and $h_0$ are the cross-sectional width and height of the main tube;d is the outer diameter of the branch tube;$b_2$ and $h_2$ are the width and length of the cover plate; $t_0$,$t_1$, and $t_2$ are the thicknesses of the main tube, branch tube, and cover plate, respectively.

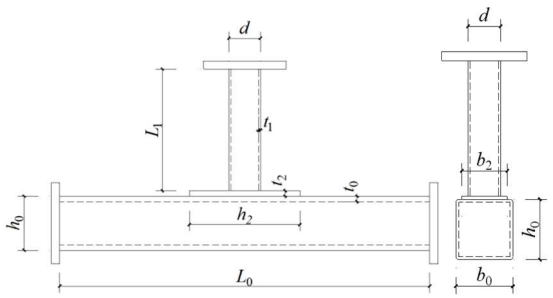


**Fig.1** Geometric Parameters of T-Joint

ISSN: 2414-1895 DOI: 10.6919/ICJE.202506_11(6).0019

## 2.2 Establishment of Finite Element Model

The finite element software ABAQUS is highly accurate in handling material and geometric nonlinearities, and thus is employed for modeling in this paper. Currently, the main element types in ABAQUS are solid elements and shell elements. Modeling with solid elements can more accurately simulate the real stress conditions of joints, though the calculation speed is relatively slow. Conversely, modeling with shell elements is faster but may neglect the influence of joint model wall thickness, potentially leading to larger calculation errors. Therefore, to balance calculation accuracy and efficiency, the solid element C3D8R is used for modeling in this study. This element can adapt to mesh deformation without loss of accuracy, well satisfying the calculation requirements.

To ensure computational accuracy while improving computational efficiency, the mesh in the doubler plate reinforced area was encrypted in this paper. Fig. 2 shows the finite element models of the unreinforced joint and the doubler plate reinforced joint. The encrypted area uses a 5mm×5mm hexahedral mesh, while the non-encrypted area uses a 20mm×20mm hexahedral mesh. It should be noted that existing studies have shown that whether to model the weld at the intersecting joint has a significant impact on the joint's stiffness and ultimate bearing capacity. Therefore, the connection weld was simulated using the solid element C3D8R in this paper.

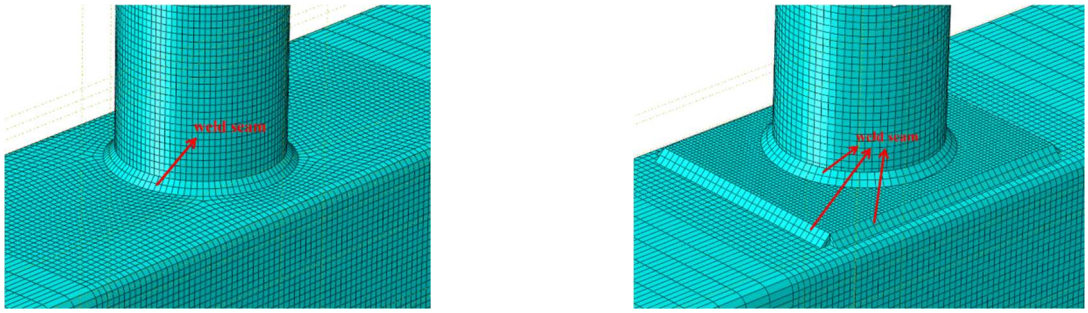


(a) Mesh at the connection of the unreinforced joint

(b) Mesh at the connection of the reinforced joint

**Fig. 2** Finite element models of the joints

In this paper, displacement loading is adopted, and supports and displacements are applied through the end nodes of the bar end elements. The boundary conditions of the main tube and branch tube are shown in Fig.3. The displacement is applied by the coupling method, that is, all the element nodes on the top surface of the branch tube are coupled to the coupling point at the center of the top surface of the branch tube. Meanwhile, the vertical degree of freedom ($U_y$) is released, and vertical displacement is applied at the coupling point to achieve the effect of applying displacement to the entire cross-section of the branch tube.

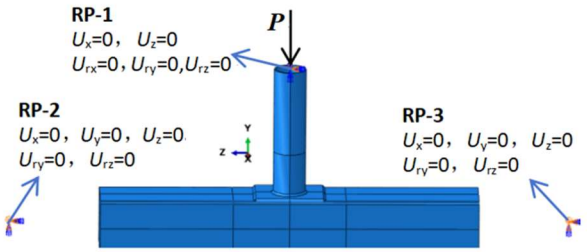


**Fig.3** Boundary conditions of T-shaped joint.

ISSN: 2414-1895 DOI: 10.6919/ICJE.202506_11(6).0019

There are two main methods for determining the ultimate bearing capacity of steel tube joints:(1)Ultimate deformation criterion: The relative deformation between the branch and main tubes reaches 3% of the side length of the main tube's cross-section;(2)Ultimate strength criterion: When the relative deformation between the branch and main tubes does not reach 3% of the main tube's cross-sectional side length, the peak point appears on the branch tube axial force-relative deformation curve.The smaller value of the two is taken as the ultimate bearing capacity of the joint [16-18]. For steel tube joints experiencing component failure, the load at the time of component failure is selected as the joint's bearing capacity in this paper.

## 2.3 Experimental Validation of Finite Element Results

To verify the reliability of the finite element calculation results, the above-mentioned finite element modeling method was used to establish models for four groups of compressed joints from the experiment in reference [19]. The finite element analysis results were then compared with the experimental results. The joint parameters of the test specimens and the finite element calculation results are shown in Table 1, while Fig. 4 presents the branch pipe axial force-relative deformation curves obtained from both finite element analysis and experiments. The comparison indicates that the errors between the finite element calculation results and the experimental results are within an acceptable range, and the branch pipe axial force-relative deformation curves show good agreement.

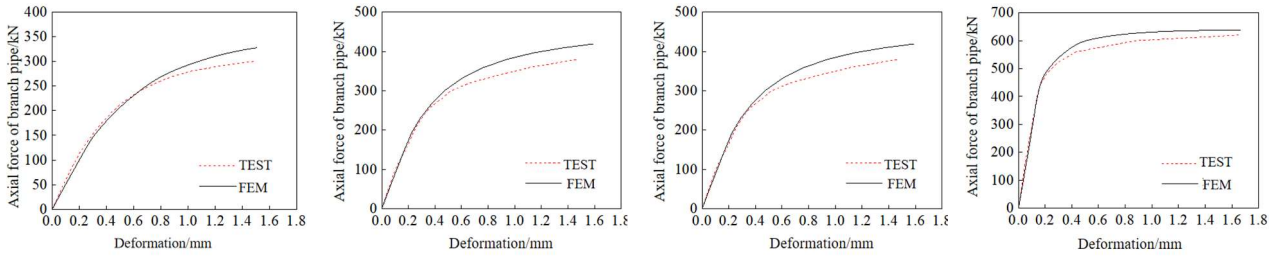


(a) CS-T1 (b) CS-T2 (c) CS-T3 (d) CS-T4

**Fig. 4** Axial force - relative deformation curve of branch pipe

Fig. 5 shows the comparison of joint failure modes between finite element analysis and experiments. As can be seen from the figure, when the branch tube is subjected to axial pressure, the upper surface of the main tube near the connection with the branch tube undergoes indentation. After loading, the maximum plastic deformation and equivalent stress of each joint are distributed on the upper wall of the main tube on both sides of the branch tube, which is consistent with the experimental phenomena [19]. Among them, due to the smaller size and lower strength of the branch tube in CS-T1, obvious buckling occurs at the root of the compressed branch tube after loading, and the joint exhibits a combined failure mode of branch tube end buckling and main tube upper wall buckling. The other three joints have larger sizes and relatively higher strengths, so no similar deformation occurs at the root of the branch tube. With the continuous increase of the load, the indentation at the connection between the main tube and the branch tube gradually increases, and local buckling appears on the side wall of the main tube. Finally, the joint fails in a mode of local buckling of the main tube upper wall and local yielding of the main tube side wall, which is consistent with the experimental phenomena [19].

ISSN: 2414-1895 DOI: 10.6919/ICJE.202506_11(6).0019

(a) Compressive branch pipe end buckling and main pipe upper wall buckling failure (CS-T1)

(b) Local buckling failure of main pipe upper wall and side wall (CS-T2)

(c) Local buckling failure of the main pipe upper wall and side wall ( CS-T3)

(d) Local buckling failure of the main pipe upper wall and side wall (CS-T4)

**Fig. 5** Comparison of joint failure modes

In summary, the finite element model established in this paper shows good agreement with the experimental results in terms of joint failure modes, deformation characteristics, and ultimate bearing capacity, and can be used to further carry out joint parameter analysis.

## 3. Parametric Analysis of Doubler Plate-Reinforced T-shaped CHS-to-SHS Joints

### 3.1 Calculation Parameters

To gain a detailed understanding of the effects of doubler plate length, width, thickness, and other factors on the failure modes and bearing capacity of joints with various geometric parameters, this section conducts a dimensionless geometric parameter analysis on the doubler plate-reinforced CHS-to-SHS T-joint based on the unreinforced joints described earlier. The dimensionless parameters used for the analysis include the branch-to-main pipe side length ratio $\beta=d/b_0$, the doubler plate width-to-main pipe side length ratio $\beta_2 = b_2/b_0$, the doubler plate-to-main pipe thickness ratio $\tau_2 = t_2/t_0$, and the doubler plate length-to-main pipe side length ratio $\alpha_2= h_2/b_0$. The material parameters of the main pipe and branch pipe are the same as those in Reference [19], and the doubler plate material is the same as that of the main pipe. In the finite element model, the elastic modulus of the steel is taken as

ISSN: 2414-1895 DOI: 10.6919/ICJE.202506_11(6).0019

$E$=2.06×10$^5$ N/mm², and the Poisson's ratio $\mu$=0.3.The parametric analysis uses a total of 4 benchmark joints and 96 doubler plate-reinforced joints, with the parameter variation scheme shown in Table 2.

**Table 1.** Joint Parameters of Test Specimens and Finite Element Analysis Results

| Test piece | Mechanical Property of | Main Pipe Specification | Branch Pipe Specification | $\beta$ | $\gamma$ | $\tau$ | Test Value | FEM Value | $N_{uc}/N_{ue}$ |
|---|---|---|---|---|---|---|---|---|---|
| CS-T1 | Compression | □200×10 | Ø89×4 | 0.445 | 20 | 0.4 | 300 | 321 | 1.07 |
| CS-T2 | Compression | □200×10 | Ø114×5 | 0.57 | 20 | 0.5 | 360 | 383 | 1.03 |
| CS-T3 | Compression | □200×10 | Ø140×6 | 0.7 | 20 | 0.6 | 490 | 556 | 1.13 |
| CS-T4 | Compression | □200×10 | Ø159×8 | 0.795 | 20 | 0.8 | 650 | 630 | 0.97 |

**Table 2.** Dimensionless parameter values of doubler plates

| $\beta$ | $\beta_2$ | $\tau_2$ | $\alpha_2$ |
|---|---|---|---|
| 0.445 | 0.8,0.9 | 0.6,0.8,1.0 | 0.8,1.0,1.2,1.6 |
| 0.57 | 0.8,0.9 | 0.6,0.8,1.0 | 0.8,1.0,1.2,1.6 |
| 0.70 | 0.8,0.9 | 0.6,0.8,1.0 | 0.8,1.0,1.2,1.6 |
| 0.795 | 0.8,0.9 | 0.6,0.8,1.0 | 0.8,1.0,1.2,1.6 |

### 3.2 Calculation Results of Finite Element Parameters

Figs 6(a)–(l) show the branch tube axial force-relative deformation curves of the doubler plate-reinforced joints, demonstrating significant strengthening effects of the doubler plates on the joints. Increasing the thickness, width, and length of the doubler plates all enhance the joint bearing capacity, with the increase in doubler plate thickness having the most pronounced effect on improving the joint bearing capacity. It can also be seen from the figures that increasing the doubler plate length can improve the joint compressive bearing capacity, but when the doubler plate length exceeds a certain value, further increasing the length hardly enhances the joint bearing capacity. For the doubler plate-reinforced joint with $\beta$=0.445, the branch tube axial force-relative deformation curve exhibits an extreme point, and yield failure of the branch tube is observed from the stress nephogram in Fig. 7(a). This is because the branch tube has a small size and thin wall thickness, and the bearing capacity of the doubler plate-reinforced joint is higher than that of the branch tube, causing the branch tube to fail before the joint. As can be seen from Figs 6(a)–(c), with the increase in doubler plate thickness, the radial stiffness of the main tube increases, and the failure mode of the joint transitions from deformation-controlled to strength-controlled. The branch tube axial force-relative deformation curves of the other three doubler plate-reinforced joints do not show obvious extreme points. However, for the doubler plate-reinforced joints with $\beta$=0.57 and some with $\beta$=0.70, the branch tube axial force-relative deformation curves cease to rise when the load reaches a certain value, indicating that the joints suffer from yield failure of the upper surface of the main tube. For the doubler plate-reinforced joints with $\beta$=0.795 and another part with $\beta$=0.70, their curves show an upward trend. The reason for this phenomenon is that the branch tubes have large diameters and thick wall thicknesses, while the radial stiffness of the main tube is increased due to the strengthening effect of the doubler plates, resulting in similar radial stiffnesses of the main tube and branch tubes. When subjected to the axial pressure of the branch tubes, the overall component displaces downward, and finally, the main tube undergoes excessive bending deformation, and the tensile stress generated at its bottom exceeds the tensile strength of the main tube, leading to failure. Such joint failures belong to component failures, indicating that the joints are excessively strengthened.

ISSN: 2414-1895 DOI: 10.6919/ICJE.202506_11(6).0019

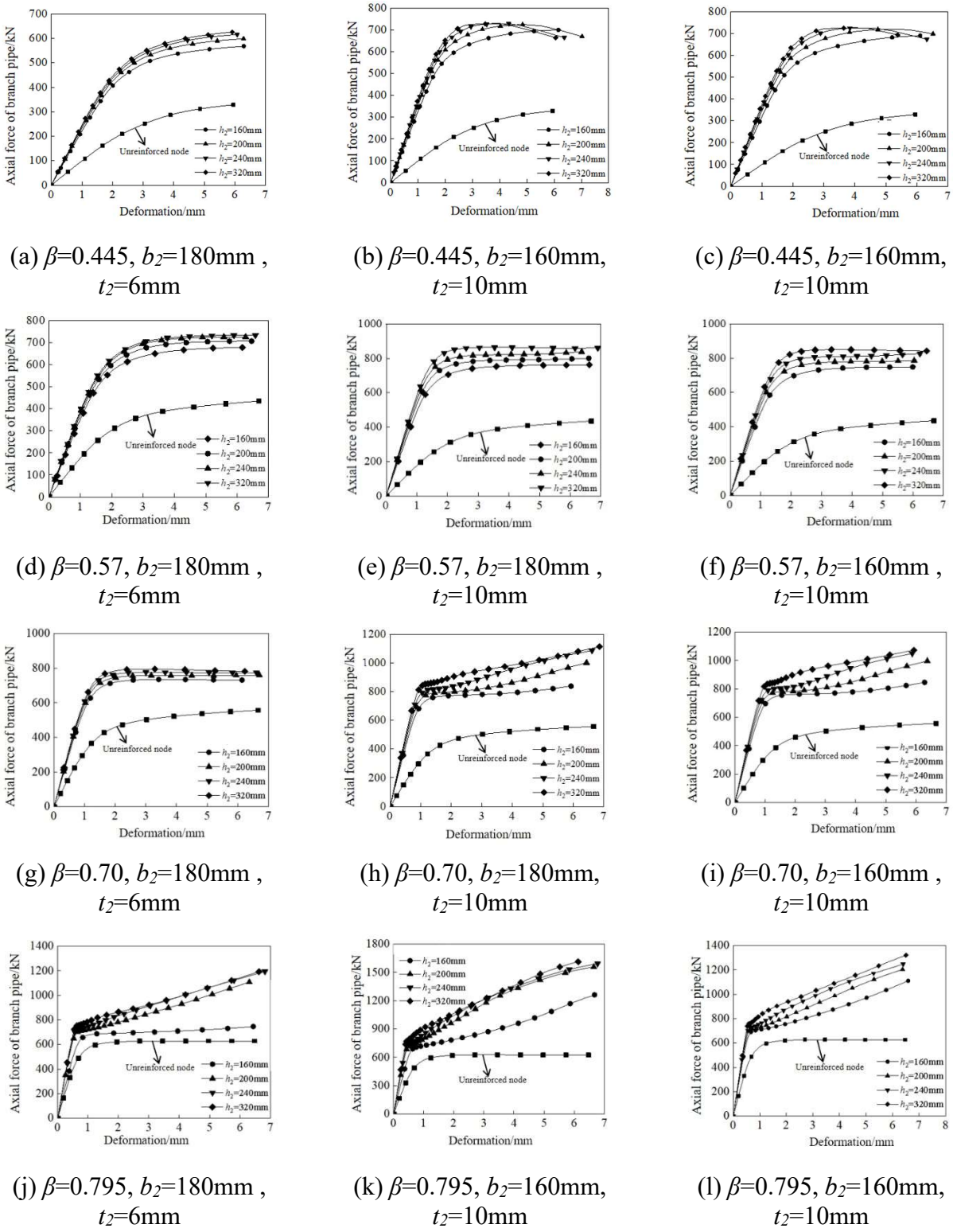


(a) $\beta$=0.445, $b_2$=180mm , $t_2$=6mm (b) $\beta$=0.445, $b_2$=160mm, $t_2$=10mm (c) $\beta$=0.445, $b_2$=160mm, $t_2$=10mm

(d) $\beta$=0.57, $b_2$=180mm , $t_2$=6mm (e) $\beta$=0.57, $b_2$=180mm , $t_2$=10mm (f) $\beta$=0.57, $b_2$=160mm , $t_2$=10mm

(g) $\beta$=0.70, $b_2$=180mm , $t_2$=6mm (h) $\beta$=0.70, $b_2$=180mm, $t_2$=10mm (i) $\beta$=0.70, $b_2$=160mm , $t_2$=10mm

(j) $\beta$=0.795, $b_2$=180mm , $t_2$=6mm (k) $\beta$=0.795, $b_2$=160mm, $t_2$=10mm (l) $\beta$=0.795, $b_2$=160mm, $t_2$=10mm

**Fig. 6** Axial force - relative deformation curve of branch pipe

### 3.3 Analysis of Joint Failure Modes

The finite element analysis results indicate that the failure modes of reinforced T-shaped square chord-to-circular brace tubular joints with cover plates can be primarily categorized into three types: brace member axial yielding failure mode (BMF), combined failure mode of brace local buckling and chord wall local buckling (BLB+CP), and combined failure mode of chord sidewall local yielding and chord wall local buckling (CSB+CP).

ISSN: 2414-1895 DOI: 10.6919/ICJE.202506_11(6).0019

Among the 96 analyzed reinforced square chord-to-circular brace tubular joints with cover plates, 24 nodes exhibited the brace member axial yielding failure mode (BMF), accounting for 25% of the total reinforced joints; 42 nodes exhibited the combined failure mode of brace local buckling and chord wall local buckling (BLB+CP), accounting for 44% of the total; and 30 nodes exhibited the combined failure mode of chord sidewall local yielding and chord wall local buckling (CSB+CP), accounting for 31% of the total. Figures 7(a) to (d) illustrate the failure modes of the reinforced T-shaped square chord-to-circular brace tubular joints with cover plates.

The brace member axial yielding failure mode (BMF) predominantly occurs in reinforced joints with β=0.445. The primary reason for this is that the width and wall thickness of the brace are significantly smaller than those of the chord. Compared to the reinforced chord, the brace has a lower load-bearing capacity. Before the brace reaches full-section yielding, the chord possesses sufficient stiffness to resist local yielding of the chord wall. In contrast to unreinforced joints, the failure mode shifts from the combined failure of chord sidewall local yielding and chord wall local buckling to brace member axial yielding, indicating that the radial load-bearing capacity of the reinforced chord far exceeds that of the brace, resulting in over-reinforcement of the joint. This failure mode is determined by observing whether the load applied to the brace at failure reaches the full-section yield load of the brace ($F=f_yA$) and by examining whether the equivalent stress in the brace cross-section, as shown in the equivalent stress cloud diagram, fully reaches the material yield stress.

The combined failure mode of brace local buckling and chord wall local buckling (BLB+CP) mainly occurs in reinforced joints with $\beta$=0.57 and $\beta$=0.70. In this failure mode, under axial load, the compressed brace experiences bulging at the end near the chord, while the chord wall at the intersection with the brace undergoes indentation. Compared to unreinforced joints, the indentation in reinforced joints is smaller, and the depression in reinforced joints follows the weld boundary between the cover plate and the upper surface of the chord, whereas in unreinforced joints, it follows the weld toe at the intersection line of the brace and chord.

The combined failure mode of chord sidewall local yielding and chord wall local buckling (CSB+CP) primarily occurs in reinforced joints with $\beta$=0.7 and $\beta$=0.795. The main cause of this failure is that when the brace is subjected to axial force, the upper wall of the chord undergoes local buckling. Since the chord surface is welded with a cover plate, the cover plate and chord jointly resist the axial force when the brace is under compression, significantly increasing the radial stiffness at the intersection of the chord and brace. However, in these joints, the brace dimensions are relatively large, and the chord wall thickness is relatively small, resulting in weak resistance to plastic deformation in the chord sidewall. As the load continues to increase, the indentation of the chord upper wall grows, simultaneously causing local buckling in the chord sidewall. Eventually, excessive bending of the chord and full-section yielding lead to structural failure.

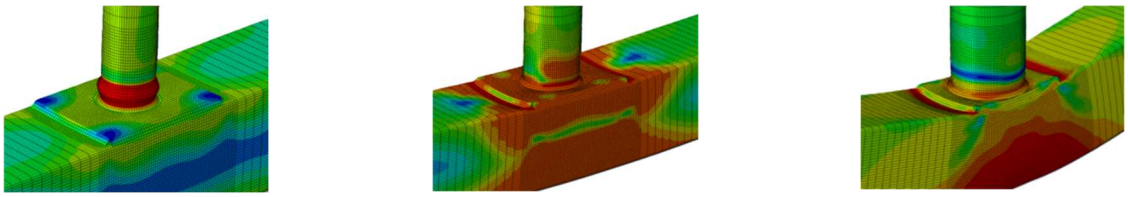

(a) BMF (b) BLB+CP (c) CSB+CP

**Fig.7** Failure modes of cover plate strengthened joints.

### 3.4 Joint Strengthening Efficiency

The axial compression ultimate bearing capacity of cover - plate strengthened joints can be determined according to the limit deformation criterion and the limit strength criterion. For the convenience of comparison, the axial compression ultimate bearing capacity of the cover - plate strengthened joint is defined as $N_{dp}$, and that of the unstrengthened joint is defined as $N_0$. The ratio of

ISSN: 2414-1895 DOI: 10.6919/ICJE.202506_11(6).0019

the two is the strengthening ratio of the joint,namely $R_{dp}=N_{dp}/N_0$. Figs 8(a)-(d) and 9 show the influence curves of the geometric parameters of the cover plate and the width ratio of the branch pipe to the main pipe on the strengthening ratio. It can be seen from the figures:① Although the width of the cover plate can improve the strengthening ratio, the improvement effect is not significant.② For the cover plates of the same size, the smaller the $\beta$, the higher the strengthening ratio. According to the plastic hinge line theory, for the unstrengthened joint, its plastic hinge line is the contour line around the weld toe. After strengthening with the cover plate, when the joint is damaged, the plastic hinge line shifts to the fillet weld around the connection between the cover plate and the surface of the main pipe, which is equivalent to increasing the total length of the plastic hinge line. For the joint with a smaller $\beta$, the size of the branch pipe is smaller, the plastic hinge line of its unstrengthened joint is shorter, and the increase in the length of the plastic hinge line after cover-plate strengthening is larger, so the strengthening ratio is higher.③ Increasing the length of the cover plate can improve the strengthening ratio. When the thickness and width of the cover plate are constant, with the increase of the length of the cover plate, the improvement of the strengthening ratio shows a trend of first fast and then slow. When the ratio of the length of the cover plate to the width of the main pipe exceeds 1.2, the strengthening ratio basically no longer increases. This is because the length of the cover plate exceeds the plastic hinge line range of the surface of the main pipe of the unstrengthened joint. Therefore, it is recommended that the length of the cover plate should not exceed 1.2 times the width of the main pipe in the design.

It can be seen from Fig 9 that for the strengthened joint with $\beta$=0.445, its strengthening ratio is large, but when the thickness of the cover plate is large, increasing the length of the cover plate has no obvious effect on improving the strengthening ratio. Based on the previous analysis, this phenomenon occurs because when the cover plate is thick, the bearing capacity of the joint and the radial stiffness of the main pipe are much greater than those of the branch pipe. Under the action of the axial force of the branch pipe, the branch pipe is damaged before the main pipe undergoes obvious deformation, and the joint is excessively strengthened. Therefore, for the strengthened joint with a smaller $\beta$, the thickness of the cover plate should not be too large. For the strengthened joint with $\beta$=0.795, when the length of the cover plate is increased from 0.8 times the width of the main pipe to 1.0 times the width of the main pipe, its strengthening ratio is improved most obviously. This is because when the length of the cover plate is increased from 0.8 times the width of the main pipe to 1.0 times the width of the main pipe, when the joint is damaged, the length of the plastic hinge line is significantly increased within the plastic hinge line range of the surface of the main pipe of the unstrengthened joint, and the strengthening ratio is obviously improved. Therefore, for the joint with a larger $\beta$, in order to ensure the strengthening effect of the cover plate, the length of the cover plate should not be less than 1.0 times the width of the main pipe.

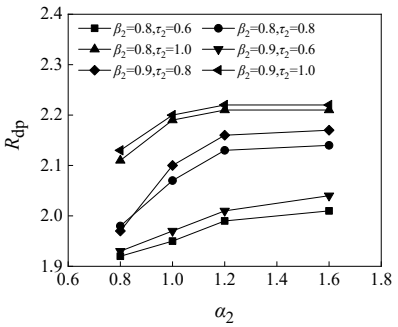


(a) $\beta$=0.445

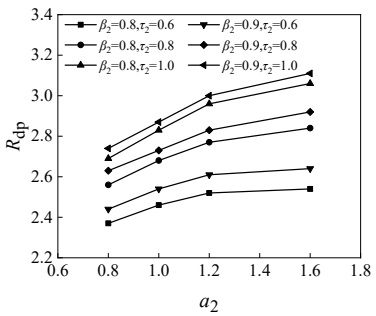


(b) $\beta$=0.57

ISSN: 2414-1895 DOI: 10.6919/ICJE.202506_11(6).0019

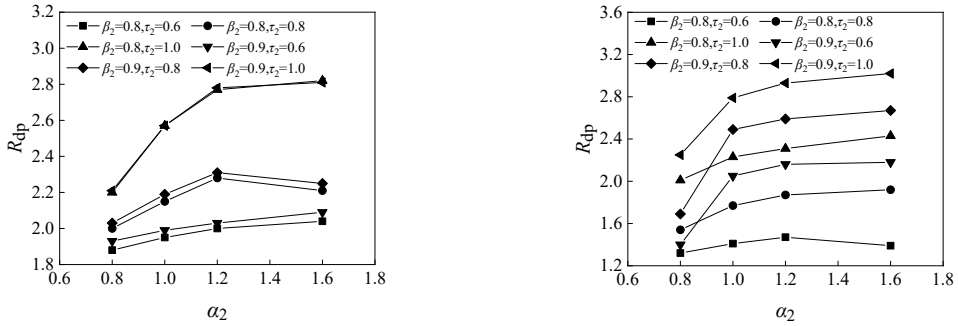


(c) $\beta$=0.70 (d) $\beta$=0.795

**Fig.8** Influence of Cover Plate Thickness and Width

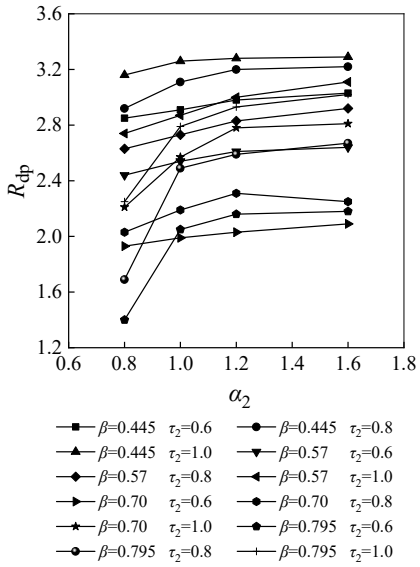


**Fig.9** Influence of Cover Plate Thickness and Branch Pipe-Main Pipe Width Ratio

# 4. Fitting of Parameter Formulas and Reliability Analysis

## 4.1 Fitting of Parameter Formulas

As indicated by the parameter analysis in the preceding sections, cover plate strengthening can significantly enhance the load-bearing capacity of rectangular main circular branch steel tubular intersecting joints. However, the current Steel Structure Design Standard(GB 50017-2017) [15] does not provide a calculation formula for this bearing capacity. Based on the standard formula and referring to the bearing capacity correction coefficient for planar K-type circular steel tubular overlap joints in Reference [20], this paper constructs the ultimate bearing capacity correction coefficient for cover plate-strengthened T-type rectangular main circular branch steel tubular intersecting joints as Equation(1):

$$\omega_0 = k_1 \beta^{k_2} \beta_2^{k_3} \tau_2^{k_4} \alpha_2^{k_5} \tag{1}$$

Where $\beta=d/b_0$, $\beta_2=b_2/b_0$, $\tau_2=t_2/t_0$, $\alpha_2=h_2/b_0$.

By combining the ratio data between the finite element analysis of cover-plate strengthened T-type rectangular main circular branch steel tubular intersecting joints and the calculation results of China's specification formulas in the preceding parameter analysis, the values of $k_1$, $k_2$, $k_3$, $k_4$, $k_5$ can be solved

ISSN: 2414-1895 DOI: 10.6919/ICJE.202506_11(6).0019

using the method of multiple linear regression, thereby obtaining the bearing capacity correction coefficient for cover-plate strengthened T-type rectangular main circular branch steel tubular intersecting joints as Equation (2):

$$\omega_0 = 2.1\beta^{-0.8}\beta_2^{0.65}\tau_2^{0.45}\alpha_2^{0.2} \tag{2}$$

Where $0.4\leq\beta\leq0.8$, $0.8\leq\beta_2\leq0.9$, $0.6\leq\tau_2\leq1.0$, $0.8\leq\alpha_2\leq1.2$.

The revised ultimate bearing capacity formula for cover-plate strengthened T-type rectangular main circular branch steel tubular intersecting joints is Equation (3):

$$N'_{cT} = \omega_0 N_{cT} \tag{3}$$

In Equation (3), the ultimate bearing capacity formula for the branch pipe compression joint is calculated according to Equation (4) summarized in China's Steel Structure Design Standard (GB 50017-2017) [15]:

$$N_{cT} = \frac{\pi}{4}\times1.8\times\frac{ft_0^{\,2}}{b_0 C\sin\theta}\left(\frac{d}{b_0 C\sin\theta}+2\right) \tag{4}$$

Where $C=(1-\beta)^{0.5}$

**Table 3.** Definitions of notations in equations (1)-(4)

| Notation | Description | Unit |
|---|---|---|
| $\beta$ | The ratio of the diameter of the branch pipe to the width of the square main pipe. | — |
| $\beta_2$ | The ratio of the width of the cover plate to the width of the square main pipe. | — |
| $\tau_2$ | The ratio of the thickness of the cover plate to the thickness of the square main pipe. | — |
| $\alpha_2$ | The ratio of the length of the cover plate to the width of the square main pipe. | — |
| $N_{cT}$ | Ultimate bearing capacity | kN |
| $N_{cT}$' | Modified ultimate bearing capacity | kN |
| $b_0$ | The side length of the square main pipe. | mm |
| $d$ | The diameter of the circular branch pipe. | mm |
| $f$ | Design strength of steel | $N/mm^2$ |
| $t_0$ | The wall thickness of the square main pipe. | mm |
| $\theta$ | The angle between the axis of the branch pipe and the axis of the main pipe. | degree |

## 4.2 Reliability Analysis of Formulas

Substituting the geometric parameter values used in the preceding parameter analysis into Equation (4), the ultimate bearing capacity correction coefficient ω0 is then compared with the ratio ω between the bearing capacity of the cover-plate strengthened joint obtained from finite element analysis and the bearing capacity of the joint calculated by the specification formula. The histogram of the ratio distribution and the statistical results are shown in Figure 10 and Table 4, respectively. It can be seen from Figure 10 and Table 4 that except for the nodes with a relatively large width ratio of branch pipe to main pipe, where the error between the calculated value of the fitting formula and the finite element analysis value is relatively large, the two are in good agreement in most cases. This indicates that the

ISSN: 2414-1895 DOI: 10.6919/ICJE.202506_11(6).0019

bearing capacity correction coefficient ω0 of the cover-plate strengthened T-type rectangular main circular branch steel tubular intersecting joint obtained by linear regression can well reflect the relative relationship between the finite element analysis value and the specification formula calculation value. The average value is slightly less than 1, and both the standard deviation and the coefficient of variation are very small, indicating that the regression formula of the bearing capacity correction coefficient of the cover-plate strengthened T-type rectangular main circular branch steel tubular intersecting joint can be used to modify the bearing capacity calculation formula of the specification.

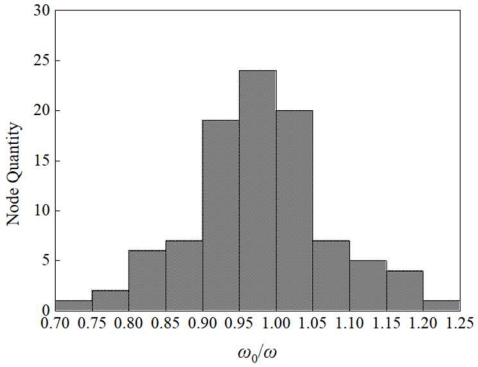


**Fig.10** Histogram of ω0/ω Distribution

**Table 4.** Statistical Table of the Ratio of Calculated Value ω0 from Fitting Formula to ω

| Node Quantity | Statistic | Statistical Value |
|---|---|---|
| 96 | Maximum value | 1.2128 |
| | Minimum value | 0.7385 |
| | Average value | 0.9742 |
| | Standard deviation | 0.0937 |
| | Coefficient of variation | 0.0962 |

## 5. Conclusion

This paper performs parametric analyses on 4 baseline joints and 96 cover plate-reinforced T-shaped tubular joints with square main tubes and circular branch tubes, investigates the influence of cover plate geometric parameters on the failure modes and ultimate bearing capacity of reinforced joints, and fits a bearing capacity design formula for such joints based on the parametric analysis results. The following conclusions are drawn:

(1) The thickness, width, and length of cover plates all affect the failure modes and load-bearing performance of joints. Increasing the cover plate thickness has the most significant effect on enhancing the joint bearing capacity, while increasing the cover plate width has the least significant effect. The joint bearing capacity first increases and then decreases with the increase of cover plate length, and the strengthening effect is optimal when $\alpha_2$=1.2.

(2) For reinforced joints with the same cover plate dimensions, smaller β values correspond to larger strengthening ratios. However, joints with extremely small or large $\beta$ values may exhibit excessive strengthening. When β is small, axial yielding failure of the branch tube may occur with increasing cover plate thickness; when β is large, failure due to full-section plasticity of the main tube may occur with increasing cover plate thickness.

(3) Based on the code formula, a bearing capacity correction factor for cover plate-reinforced T-shaped tubular joints with square main tubes and circular branch tubes is obtained through linear

ISSN: 2414-1895 DOI: 10.6919/ICJE.202506_11(6).0019

regression, and a bearing capacity calculation formula for such joints is proposed. Through regression verification of the correction factor formula, the accuracy of the proposed formula is validated.

## Acknowledgments

Hunan Provincial Natural Science Foundation Project (2023JJ31013);

Hunan Provincial College Student Innovation Training Program Project (S202310538059);

Hunan Provincial Postgraduate Scientific Research Innovation Project (CX20230740).

## References

[1] Y. Zhao, S.W. Li, Y.X. Huang, et al. Experimental study on strengthening T-shaped circular steel tube joints with external stiffeners [J]. China Civil Engineering Journal, 2014, 47(09): 70-75. (in Chinese).

[2] T. Li, Y.B. Shao, J.C. Zhang. Static strength study on reinforced pipe joints with built-in vertical inserts [J]. Engineering Mechanics, 2010, 27(04): 133-140. (in Chinese).

[3] H.F. Chang, W. Xu, W.K. Zuo, et al. Analysis of compressive bearing performance of square steel tube joints strengthened with vertical inserts [J]. Journal of Central South University (Science and Technology), 2019, 50(09): 2242-2251. (in Chinese).

[4] H.F. Chang, J.W. Xia, X.M. Duan, et al. Static compression test on T-shaped joints of square steel tubes strengthened with cover plates and vertical inserts [J]. Journal of Building Structures, 2013, 34(10): 57-63. (in Chinese).

[5] H.F. Chang, T.L. Ren, R. Zhang, et al. Research progress on axial mechanical properties of square steel tube joints strengthened with backing plates/ring plates [J]. Progress in Steel Building Structures, 2022, 24(06): 1-10-19. (in Chinese).

[6] L.Q. Wu, Z.L. Li, Q.H. Han. Experimental study on static performance of backing plate-strengthened N-shaped circular steel tube joints [J]. Journal of Building Structures, 2010, 31(10): 83-88. (in Chinese).

[7] H.F. Chang, J.W. Xia, H. Chang, et al. Compressive bearing mechanism of T-shaped joints of square steel tubes strengthened with cover plates [J]. Journal of South China University of Technology (Natural Science Edition), 2013, 41(06): 77-83. (in Chinese).

[8] X.P. Shu, X. Zhang, Z.S. Yuan. Study on ultimate compressive bearing capacity of backing plate-strengthened Y-shaped circular steel tube joints [J]. Building Structure, 2009, 39(09): 87-90. (in Chinese).

[9] Z.L. Li, L.Q. Wu, B. Zhu, et al. Experimental comparison of mechanical properties of N-shaped circular steel tube joints under different strengthening measures [J]. Engineering Mechanics, 2008, (11): 179-185. (in Chinese).

[10] FENG R,CHENY,CHEND F.Experimental and numerical investigations on collar plate and doubler plate reinforced SHST-joints under axial compression[J].Thin-Walled Structures,2017,1 10:75-87.

[11] SOH C K,CHAN T K,FUNG T C.Ultimate capacity of doubler plate reinforced square hollow section T-joints(mechanics,strength&structure)[J].Transactions of Joiningand Welding Research Institute of Osaka University,2000,29(2)85-90.

[12] W.J. Wang, Y.B. Shao, H. Xia. Study on the Ultimate Bearing Capacity of T-shaped Square Steel Tube Joints Strengthened with Ring Plates Under Axial Compression [J]. Engineering Mechanics, 2012, 29(06): 138-145. (in Chinese).

[13] W.J. Wang, Y.B. Shao. Parametric Analysis of the Ultimate Bearing Capacity of T-shaped Square Steel Tube Joints Strengthened with Ring Plates Under Axial Compression [J]. Journal of Civil Engineering and Management, 2011, 28(02): 32-38. (in Chinese).

[14] Y.Q. Cai, Y.B. Shao, Y.S. Yue. Experimental Study on the Bearing Capacity of Ring Plate-reinforced T-shaped Circular Steel Tube Joints [J]. Engineering Sciences, 2011, 28(09): 90-94+102. (in Chinese).

[15] Code for Design of Steel Structures: GB 50017-2017 [S]. Beijing: China Architecture & Building Press, 2018. (in Chinese).

[16] Yura J A, Zettlemoyer N, Edwards I F. Ultimate capacity of circular tubular joints[J]. Journal of the structural division, 1981, 107(10): 1965-1984.

ISSN: 2414-1895 DOI: 10.6919/ICJE.202506_11(6).0019

[17] L H Lu, G D De Winkel, Y Yu, et al. Deformation limit for the ultimate strength of hollow section joints[C]. 6th International Symposium on Tubular Structures, 1994. 341-347.

[18] Z.Y. Che, Y.F. Tian, X.X. Ma. Finite Element Analysis on the Bearing Capacity of T-shaped Joints with Circular Main Tubes and Square Branch Tubes [J]. Building Structure, 2011, 41(S1): 853-856. (in Chinese).

[19] Y. Gan. Study on the Mechanical Behavior of T-shaped Concrete-Filled Steel Tube Joints with Square Main Tubes and Circular Branch Tubes Made of High-Strength Steel [D]. Central South University of Forestry and Technology, 2022. (in Chinese).

[20] Y. Chen. Study on the Static Performance of Planar K-type Overlapped Circular Steel Tube Joints [D]. Tongji University, 2006. (in Chinese).